14th International Symposium on Turbulence and Shear Flow Phenomena (TSFP14)
Heidelberg, Germany, July 28–31, 2026

# UNSTEADY PERTURBATIONS IN TWO-DIMENSIONAL TURBULENCE

**Guoyu Fan & Wouter J.T. Bos**

Laboratoire de Mécanique des Fluides et d'Acoustique (LMFA)
CNRS, Ecole Centrale de Lyon, INSA Lyon, Université Claude Bernard Lyon 1,
69134 Écully, France
*guoyu.fan@ec-lyon.fr*

## ABSTRACT

Equilibrium can be defined as the balance between production and dissipation of a given quantity. Whereas in 3D turbulence, a relevant quantity is the kinetic energy, for the case of 2D turbulence for scales smaller than the forcing, the most pertinent quantity is the enstrophy. Small non-equilibrium corrections can then be accurately described by linear perturbation around this equilibrium. We illustrate this for the total enstrophy spectrum using Direct Numerical Simulations and for its spectrum using Spectral Closure integration.

## 1 INTRODUCTION

Turbulence is characterized by spatio-temporal fluctuations at a range of different length and timescales. The distribution over lengthscales is a result of the nonlinear coupling of modes, resulting, in 3D, in a cascade of energy among scales. Kolmogorov's 1941 theory predicts a constant energy flux through the inertial range, leading to the well-known spectrum $E(k) \sim k^{-5/3}$ (Kolmogorov, 1941). In contrast, the two-dimensional case exhibits a dual cascade: an inverse transfer of energy towards large scales, and a forward enstrophy cascade with spectrum of the form $E(k) \sim k^{-3}$ (Kraichnan, 1967; Batchelor, 1969).

In fluctuating (turbulent) flows it is of practical importance to distinguish between equilibrium and non-equilibrium contributions. Whereas equilibrium can be described by well-established (engineering) models, non-equilibrium is not always taken into account. In a recent series of investigations (Fang & Bos, 2023; Bos, 2024; Bos & Araki, 2025; Araki & Bos, 2024), we showed how linear perturbation can be applied to estimate both spatial and temporal non-equilibrium in 3D turbulence.

The two-dimensional case has received far less attention, but we can mention the application of the ideas to surface quasi-geostrophic turbulence (Valadão *et al.*, 2024). The present investigation focuses on the 2D Navier-Stokes equations and shows how non-equilibrium affects the statistics of turbulent quantities in the enstrophy cascade. For this we will extend the theoretical approach developed for 3D turbulence to the two-dimensional case. Ideas will be tested using high-resolution direct numerical simulations (DNS) and closure theory of the eddy-damped quasi-normal Markovian (EDQNM) type.

## 2 ENSTROPHY STATISTICS IN TWO-DIMENSIONAL TURBULENCE

The enstrophy balance in two-dimensional turbulence in a closed or spatially periodic domain can be written as

$$\frac{\mathrm{d}Z(t)}{\mathrm{d}t} = P_\Omega(t) - \chi(t), \tag{1}$$

where $Z(t) = \frac{1}{2}\int \omega^2(\boldsymbol{x},t)\,\mathrm{d}\boldsymbol{x}$ denotes the total enstrophy, $P_\Omega(t)$ is the enstrophy injection rate due to external forcing, and $\chi(t)$ is the enstrophy dissipation rate associated with viscosity.

Equilibrium in two-dimensional turbulence refers to the condition in which the enstrophy injection by external forcing balances the viscous enstrophy dissipation, $P_\Omega(t) = \chi(t)$. This balance underlies the derivation of inertial-range scaling laws, in particular the Batchelor–Kraichnan prediction for the forward enstrophy cascade, $Z(k) \equiv k^2E(k) \sim k^{-1}$, including its logarithmic correction (Kraichnan, 1971). The enstrophy spectrum is defined such that

$$\int Z(k,t)dk = Z(t). \tag{2}$$

Non-equilibrium states arise when, globally, temporal variations of the enstrophy flux induce deviations from the equilibrium state. In 3D turbulence these fluctuations give rise to sub-dominant corrections to the energy spectrum $E(k,t)$ proportional to $k^{-7/3}$ (Yoshizawa, 1994; Woodruff & Rubinstein, 2006; Bos & Rubinstein, 2017). We now discuss the case in two dimensions.

We start from the promise that departure from equilibrium can be described as small perturbations, defined by the difference between the total spectrum $Z(k,t)$ and its equilibrium part. Accordingly, the enstrophy spectrum can be expanded as

$$Z(k,t) = Z_0(k,t) + Z_1(k,t) + Z_2(k,t) + \cdots, \tag{3}$$

where $Z_1, Z_2, \ldots$ represent successive non-equilibrium corrections. Under equilibrium conditions, the enstrophy injection balances the enstrophy dissipation, i.e. $P_\Omega(t) = \chi(t)$. Based on this balance, we assume that the leading-order enstrophy spectrum ignoring logarithmic corrections (Kraichnan, 1971) takes the form

$$Z_0(k,t) = C_\Omega\,\chi(t)^{2/3}k^{-1}, \tag{4}$$

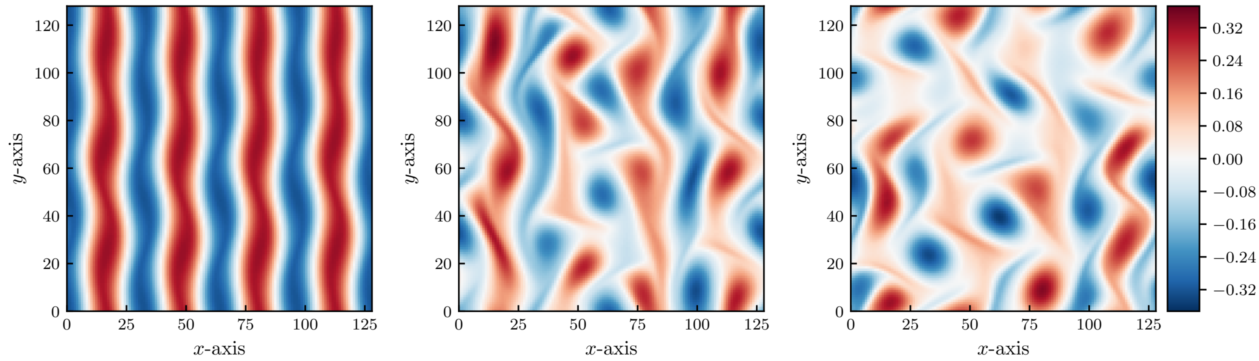


(a) (b) (c)

Figure 1. Visualization of the two-dimensional vorticity field in Kolmogorov flow at early developments (a) $t = 144$, (b) $t = 384$, and at turbulent state (c) $t = 1604$.

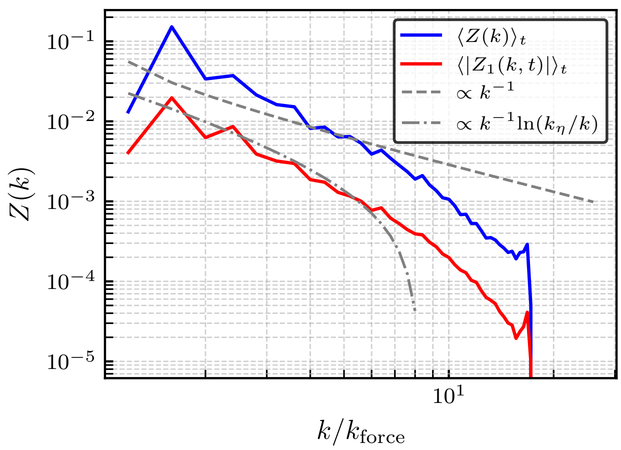


Figure 2. Time-averaged enstrophy spectra in the nonequilibrium turbulent regime over $1000 \le t \le 4000$: total enstrophy spectrum and first-order perturbation enstrophy spectrum.

where $C_\Omega$ is a constant. Furthermore, regarding $Z_i(k,t)$ as the $i$-th order perturbation of the enstrophy spectrum. Following Horiuti & Tamaki (2013), for 3D turbulence, the procedure to obtain higher-order corrections then amounts to solving a recursive form of the local enstrophy balance equation, written as

$$\int_k^{k_\eta} \left( \frac{\partial Z_i(k',t)}{\partial t} \right) \mathrm{d}k' = \frac{3}{2} \frac{Z_{i+1}(k,t)}{Z_0(k,t)} \chi(t). \tag{5}$$

Each perturbative contribution $Z_{i+1}(k,t)$ can be determined recursively from the temporal evolution of the preceding term $Z_i(k,t)$, thereby establishing a systematic expansion around the equilibrium solution. Using a simplified model for two-dimensional turbulence, the first two perturbative predictions of the enstrophy spectrum can be expressed as

$$Z_1(k,t) \propto \dot{\chi}(t)\,\chi(t)^{-2/3}\,k^{-1}\,\ln\left(\frac{k_\eta}{k}\right), \tag{6a}$$

$$Z_2(k,t) \propto \left(\ddot{\chi}(t)\,\chi(t)^{-1} - \tfrac{2}{3}\dot{\chi}^2(t)\,\chi(t)^{-2}\right) k^{-1}\,\ln^2\left(\frac{k_\eta}{k}\right), \tag{6b}$$

where $\dot{\chi}(t)$ and $\ddot{\chi}(t)$ denote the first and second time derivatives of the enstrophy dissipation rate, respectively.

## 3 RESULTS FOR ENSTROPHY SPECTRUM

Direct numerical simulations were performed with the pseudo-spectral GHOST code. The spatial resolution was $128^2$, corresponding to Fourier modes $k_x, k_y \in [-64, 64]$. The kinematic viscosity was fixed at $\nu = 10^{-4}$. Time advancement was performed using a second-order Runge–Kutta scheme with a time step $\Delta t = 10^{-4}$. A large-scale linear friction term was included, and the flow was driven by a deterministic Kolmogorov forcing, i.e. a sinusoidal body force applied at wavenumber $k_f = 4$. In physical space, the forcing is given by

$$\vec{f}(\vec{x},t) = -f_0 \sin(k_f x)\vec{e}_y, \tag{7}$$

with $f_0 = 20$.

Figure 1 illustrates the early-stage evolution of the vorticity field in the Kolmogorov flow. In figure 1(a), the flow is still dominated by the nearly sinusoidal banded structure imposed by the forcing. In figure 1(b), the bands become significantly deformed, indicating the amplification of perturbations and the onset of instability. In figure 1(c), more evident roll-up and coherent vortical structures appear.

After $t \gtrsim 1000$, the flow enters a nonequilibrium turbulent regime. In this stage, the total kinetic energy fluctuates around $\bar{E} \approx 1.2 \times 10^{-3}$. We obtain $\mathscr{U} \sim \sqrt{2\bar{E}} = 4.9 \times 10^{-2}$. Taking the forcing length scale as $\mathscr{L} = 1/k_f = 1/4$, the corresponding Reynolds number is estimated as

$$Re = \frac{\mathscr{U}\mathscr{L}}{\nu} = 1.2 \times 10^2. \tag{8}$$

We then apply the perturbation decomposition (6) to the flow fields and perform a time average over the interval $1000 \le t \le 4000$. The resulting averaged spectra are shown in figure 2. A comparison of the total enstrophy spectrum with the first-order perturbation spectrum shows that the latter remains approximately one order of magnitude smaller over most of the resolved wavenumber range. While this suggests that the first-order correction makes a measurable contribution, the spectrum does not allow to validate prediction (6).

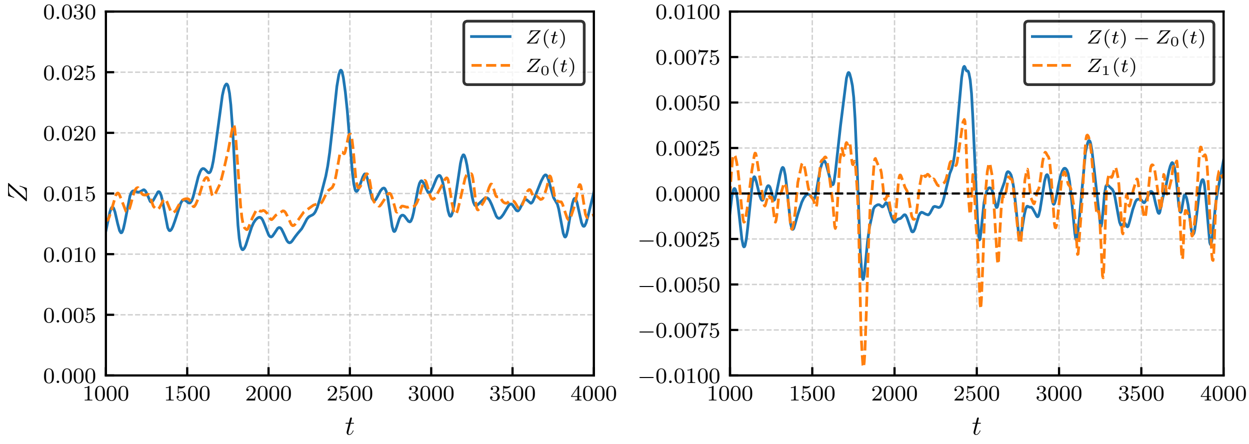


(a) (b)

Figure 3. (a) Time evolution of the total enstrophy $Z$ and the leading-order estimate $Z_0$. (b) Comparison between the numerical first-order correction $Z-Z_0$ and the theoretical prediction of $Z_1$.

## 4 PREDICTION FOR INTEGRAL QUANTITIES

The numerical results do not allow to assess the prediction for the spectra. However, as we will show, they do allow to validate a perturbation approach applied to the integral, global value, of the enstrophy. To connect this spectral perturbation expansion with the global quantities (Enstrophy, Kinetic energy). Following Taylor's statistical theory of turbulence (Taylor, 1935), we estimate the characteristic transfer time as $\tau \sim \mathscr{L}/\mathscr{U}$. In its original form, this argument provides a stationary scaling estimate and does not explicitly involve time dependence. Recently, Bos and Araki (Bos & Araki, 2025) analyzed equilibrium and nonequilibrium statistics in inhomogeneous and unsteady three-dimensional turbulence using an equilibrium-plus-perturbation decomposition, and showed that the perturbative correction is linked to temporal variations of the flow. In the present unsteady two-dimensional context, we therefore extend Taylor's idea in an instantaneous sense by allowing the characteristic quantities $\mathscr{U}$, $\mathscr{L}$, and $Z$ to vary with time. This leads to the time-dependent estimate

$$\chi(t) = C'_\Omega \frac{\mathscr{U}(t) Z(t)}{\mathscr{L}}, \tag{9}$$

where $C'_\Omega$ is a new dimensionless constant.

In the present work, the leading-order equilibrium contribution is estimated directly from the dissipation rate. Thus,

$$\chi(t) = C'_\Omega \frac{\mathscr{U}(t) Z_0(t)}{\mathscr{L}}, \tag{10}$$

so that

$$Z_0(t) = \frac{\chi(t)\mathscr{L}}{C'_\Omega \mathscr{U}(t)}. \tag{11}$$

The first-order non-equilibrium correction is then defined as

$$Z_1(t) = Z(t) - Z_0(t). \tag{12}$$

Here, $Z_0(t)$ should be understood as a dissipation-based estimate of the leading-order equilibrium enstrophy over the range $[k_f, k_\eta]$ which balance $P_\Omega(t)$ and $\chi(t)$, and $Z_1(t)$ measures the departure from this equilibrium state. Using first-order perturbation theory, combining (1) and (3) we write

$$\frac{\mathrm{d}Z_0(t)}{\mathrm{d}t} = P_\Omega(t) - C'_\Omega \frac{\mathscr{U}(t)}{\mathscr{L}} \left[ Z_0(t) + Z_1(t) \right], \tag{13}$$

yielding, using (11)

$$Z_1(t) = \frac{1}{\mathscr{U}(t)} \frac{\mathrm{d}}{\mathrm{d}t} \left[ \frac{\chi(t)}{\mathscr{U}(t)} \right] \frac{\mathscr{L}^2}{C'^2_\Omega}. \tag{14}$$

In figure 3 we compare the predictions to the results of the DNS.

As shown in figure 3(a), the leading-order estimate $Z_0$ follows the overall evolution of the total enstrophy $Z$, but with a smaller fluctuation amplitude and a noticeable time lag. This indicates that the equilibrium approximation captures only the dominant trend of the enstrophy dynamics. In figure 3(b), the theoretical first-order correction $Z_1$ is seen to evolve in close synchrony with the difference $Z - Z_0$. The remaining deviations between the two is therefore attributed to the influence of higher-order terms.

## 5 RESULTS AT HIGH REYNOLDS NUMBER

The observations shown in figure 3 validate the perturbation approach. However, a more refined analysis of the enstrophy spectra requires much higher resolution. Indeed, figure 2 showed that the present resolution is not sufficient to validate the perturbation approach applied to the spectra. To assess the spectral perturbation theory more efficiently, we therefore employ the EDQNM model, which was previously shown to validate the 3D case (Fang & Bos, 2023). We examine the results of EDQNM integration for the case of periodically forced two-dimensional turbulence. Figure 4 shows that this approach yields a perturbation spectrum which, at leading order, is in agreement with our theoretical prediction. In particular, the EDQNM results provide clearer evidence for the first-order unsteady correction than the DNS data at the present resolution, and therefore offer additional support for the perturbation analysis. We note here that the results obtained here, if they were

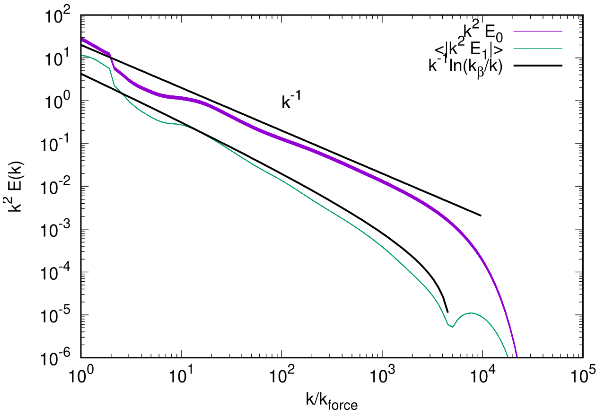


Figure 4. Results obtained using the EDQNM closure model. In this figure, $E_0$ is the equilibrium energy spectrum, $E_1$ the unsteady correction, and $k_\beta$ is the viscous scale.

to be produced by DNS, would need a prohibitively high resolution of $N_x \times N_y \approx (10^5)^2$ grid-points to attain a comparable scale separation.

## REFERENCES

Araki, Ryo & Bos, Wouter J. T. 2024 Inertial range scaling of inhomogeneous turbulence. *Journal of Fluid Mechanics* **978**, A9.

Batchelor, George K 1969 Computation of the energy spectrum in homogeneous two-dimensional turbulence. *The Physics of Fluids* **12** (12), II–233.

Bos, Wouter JT 2024 Unsteady and inhomogeneous turbulent fluctuations around isotropic equilibrium. *Atmosphere* **15** (5), 547.

Bos, Wouter JT & Araki, Ryo 2025 Equilibrium and nonequilibrium statistics in inhomogeneous and unsteady turbulence. *Physical Review Fluids* **10** (4), 044603.

Bos, Wouter JT & Rubinstein, Robert 2017 Dissipation in unsteady turbulence. *Physical Review Fluids* **2** (2), 022601.

Fang, Le & Bos, Wouter JT 2023 An edqnm study of the dissipation rate in isotropic non-equilibrium turbulence. *Journal of Turbulence* **24** (6-7), 217–234.

Horiuti, Kiyosi & Tamaki, Takahiro 2013 Nonequilibrium energy spectrum in the subgrid-scale one-equation model in large-eddy simulation. *Physics of Fluids* **25** (12).

Kolmogorov, Andrey Nikolaevich 1941 The local structure of turbulence in incompressible viscous fluid for very large reynolds. *Numbers. In Dokl. Akad. Nauk SSSR* **30**, 301.

Kraichnan, Robert H 1967 Inertial ranges in two-dimensional turbulence. *Tech. Rep.*.

Kraichnan, Robert H 1971 Inertial-range transfer in two-and three-dimensional turbulence. *Journal of Fluid Mechanics* **47** (3), 525–535.

Taylor, G. I. 1935 Statistical theory of turbulence. *Proceedings of the Royal Society of London. Series A, Mathematical and Physical Sciences* **151** (873), 421–444.

Valadão, VJ, Ceccotti, T, Boffetta, G & Musacchio, S 2024 Nonequilibrium fluctuations of the direct cascade in surface quasi-geostrophic turbulence. *Physical Review Fluids* **9** (9), 094601.

Woodruff, Stephen L & Rubinstein, Robert 2006 Multiple-scale perturbation analysis of slowly evolving turbulence. *Journal of Fluid Mechanics* **565**, 95–103.

Yoshizawa, Akira 1994 Nonequilibrium effect of the turbulent-energy-production process on the inertial-range energy spectrum. *Physical review E* **49** (5), 4065.